DRAL
Daresbury Laboratory
Rutherford Appleton Laboratory

RAL Report
RAL-94-120

Minijet Vito: a Tool for the Heavy Higgs Search at the LCH

V Barger, RJN Phillips and D Zeppenfeld

January 1995

Rutherford Appleton Laboratory Chilton DIDCOT Oxfordshire OX11 0QX

Rutherford Appleton Laboratory

MAD/PH/856

RAL-94-120

December 1994

Minijet veto: a tool for the heavy Higgs search at the LHC

V. Barger,[1] R. J. N. Phillips[2], D. Zeppenfeld[1]

[1] *Department of Physics, University of Wisconsin, Madison, WI 53706*

[2] *Rutherford Appleton Laboratory, Chilton, Didcot, Oxon, England*

ABSTRACT

The distinct color flow of the $qq \to qqH$, $H \to W^+W^-$ process leads to suppressed radiation of soft gluons in the central region, a feature which is not shared by major background processes like $t\bar{t}$ production or $q\bar{q} \to W^+W^-$. For the leptonic decay of a heavy Higgs boson, $H \to W^+W^- \to \ell^+\nu\ell^-\bar{\nu}$, it is shown that these backgrounds are typically accompanied by minijet emission in the 20–40 GeV range. A central minijet veto thus constitutes a powerful background rejection tool. It may be regarded as a rapidity gap trigger at the semihard parton level which should work even at high luminosities.

I. INTRODUCTION

Finding ways to detect a heavy Higgs boson or longitudinal weak boson scattering at the LHC is an issue of highest importance as long as the nature of spontaneous electroweak symmetry breaking remains to be established. Over the past few years considerable work has been devoted to this topic and several techniques have been proposed to separate the signals from large backgrounds due to QCD processes and/or the production of W bosons from the decay of top quarks. In order to identify weak boson scattering, *i.e.* the electroweak subprocess $qq \to qqVV$, tagging of at least one fast forward jet is essential [1]. Early studies [2–5] showed that double tagging is quite costly to the signal rate because one of the two quark jets has substantially lower median p_T (order 30 GeV) than the other (order 80 GeV). Single forward jet tagging relies only on the higher p_T tag-jet and thus proves an effective technique [5–8].

A study of the WW signal must exploit additional identifying characteristics. For example, the W bosons from top quark decays can be rejected by vetoing the additional central b quark jets arising in $t \to Wb$ [4,6]. In case of the decay $H \to W^+W^- \to \ell^+\nu\ell^-\bar{\nu}$ another important discriminator is a large transverse momentum difference between the charged leptons [8].

In a weak boson scattering event no color is exchanged between the initial state quarks. Color coherence between initial and final state gluon bremsstrahlung then leads to a suppression of hadron production in the central region, between the two tagging jet candidates of the signal [9–11]. It was hoped that the resulting rapidity gaps (large regions in pseudorapidity without observed hadrons apart from the Higgs decay products) could be used to select signal events. However, at LHC energies the low signal cross sections require running at high luminosity and then overlapping events in a single bunch crossing will likely fill a rapidity gap even if it is present at the level of a single pp collision.

In the present paper, we argue that the rapidity gap idea may be rescued at LHC energies if we look for gaps in minijet production rather than gaps in soft hadron production. The gluon radiation in background events is hard enough to lead to a characteristic minijet pattern which provides an experimentally accessible measure of the color flow in the underlying hard event.

Qualitatively, extra parton emission is suppressed by a factor $f_s = \alpha_s ln\,(Q^2/p_{T,min}^2)$, where Q is the typical scale of the hard process and $p_{T,min}$ is the minimal transverse momentum required for a parton to qualify as a minijet. The jet transverse momentum scale below which multiple minijet emission must be expected is set by $f_s = 1$. In the background processes for a heavy Higgs boson the relevant hard scale may be as large as the Higgs mass (*i.e.* W^+W^- invariant mass). Setting $Q = 1$ TeV, $f_s = \mathcal{O}(1)$ may be expected for $p_{T,min} = \mathcal{O}(30\ GeV)$. Multiple minijet emission at such a high scale should be observable even in a high luminosity environment and therefore be useful as an event selection criterion.

As a case study to quantify these arguments, we consider the decay mode $H \to W^+W^- \to \ell^+\nu\ell^-\bar{\nu}$ of a heavy Higgs boson (typically $m_H = 800$ GeV). Our first goal is to make a more reliable estimate of the typical transverse momentum scale and the rapidity range at which individual background events develop a high probability for minijet activity. Second we establish that such minijets are unlikely to be observed in signal events. Hence, a veto on these minijets should constitute a powerful tool to isolate a heavy Higgs boson or more generally a weak boson scattering signal. Finally, we give numerical results for a typical search strategy at the LHC. We demonstrate that backgrounds may be reduced well below the signal level while retaining a sizable signal (80 events for $m_H = 800$ GeV and an integrated luminosity of 100 fb^{-1}) if a minijet veto above $p_T = 20$ GeV is possible.

II. CALCULATIONAL TECHNIQUES

At least two features of soft parton emission in a hard process must be reliably modeled in order to answer the questions raised above: i) The color flow of the hard process and the ensuing color coherence of the soft radiation needs to be taken into account. ii) The hard scale Q, which determines the transverse momentum region where multiple minijet emission sets in, must be determined dynamically. Both requirements are satisfied by a full evaluation of tree level matrix elements, including the radiation of one additional soft parton. Fortunately, Monte Carlo programs for all the necessary signal and background simulations exist already.

Since we are interested in heavy Higgs boson production, a simulation using the narrow Higgs width approximation is inadequate. Instead we evaluate the full electroweak subprocesses

$$qQ \quad \rightarrow \quad qQ \; W^+W^- + n\,g \quad \rightarrow \quad qQ \; \ell^+\nu\ell^-\bar{\nu} + n\,g \tag{1}$$

(and corresponding crossing related ones) including all W-bremsstrahlung diagrams. The W decays are generated in the narrow width approximation. For the lowest order case with no gluon emission (n = 0) we use the calculation described in Ref. [6]. In order to determine the soft parton radiation pattern for the signal we calculate the signal cross section for n = 1 gluon as described in Ref. [12]. In all cases we choose the scale Q of the structure functions and of $\alpha_s(Q^2)$ to be the smallest individual parton transverse momentum in the final state. For all processes we use MRS A structure functions [13] and we set $\alpha_s(m_Z^2) = 0.12$.

A forward tagging jet, well separated from the W decay leptons, will be part of the signal definition. Even in the top quark background such an additional jet will almost always be produced by QCD radiation and not by the b-quark arising in $t \rightarrow Wb$ decay. Hence the lowest order $t\bar{t}$ background is given by subprocesses like

$$q\bar{q},\; gg \rightarrow t\bar{t}g, \quad with \quad t\bar{t} \rightarrow W^+W^-b\bar{b} \rightarrow \ell^+\nu\ell^-\bar{\nu}b\bar{b}\,. \tag{2}$$

The corresponding simulation (called $t\bar{t}j$ Monte Carlo in the following) is based on the cross section formulas given in Ref. [14]. When considering the minijet activity, the top background needs to be determined with one additional parton in the final state and we use a tree level $\mathcal{O}(\alpha_s^4)$ Monte Carlo program ($t\bar{t}jj$ Monte Carlo) which includes the subprocesses

$$gg \rightarrow t\bar{t}gg\,, \tag{3}$$

$$q\bar{q} \rightarrow t\bar{t}gg\,, \tag{4}$$

$$qQ \rightarrow t\bar{t}qQ \tag{5}$$

and all crossing related ones, but which neglects Pauli interference terms when identical quark flavors are appearing in the six quark process [15]. Neglecting Pauli interference is an excellent approximation since we are interested in the phase space region where the two final state massless

partons have very different transverse momenta and energies. In both the $t\bar{t}j$ and $t\bar{t}jj$ Monte Carlos the top quark and W decays are simulated in the narrow width approximations. In addition, energy loss from unobserved neutrinos in semileptonic b-quark decays is simulated by appropriately decreasing the 3-momentum of the corresponding jet. In both programs the minimal E_T of the final state partons, prior to top quark decay, is chosen as the scale of the structure functions. For the overall strong coupling constant factors we take $\alpha_s^3 = \alpha_s(E_T(t))\,\alpha_s(E_T(\bar{t}))\,\alpha_s(p_T(j))$ and $\alpha_s^4 = \alpha_s(E_T(t))\,\alpha_s(E_T(\bar{t}))\,\alpha_s(p_T(j_1))\,\alpha_s(p_T(j_2))$, respectively (where $E_T^2 = p_T^2 + m^2$). The top quark mass is set to $m_t = 174$ GeV throughout.

Similar to the top quark background, the QCD W^+W^- background is simulated with $n = 0$ to $n = 2$ final state quarks or gluons and is generated by a full evaluation of all α_s^n tree level subprocesses [16]. Full 1-loop corrections are only known for inclusive W^+W^- production and we effectively include them by a factor $K = 1.68$ for the $n = 0$ process [17]. This large K-factor is partially due to the emergence of new subprocesses at the $n = 1$ level and therefore is not used for the $n = 1$ and $n = 2$ simulations. The W decays are again treated in the narrow width approximation, the strong coupling constant factors are taken as $\alpha_s^n = \Pi_{i=1}^n \alpha_s(p_T(j_i))$, *i.e.* each α_s is evaluated at the transverse momentum of the corresponding final state parton, and the smallest E_T of the W's or jets is taken as the structure function scale.

Below we will be interested in using the higher order programs (which include emission of soft partons) in regions of phase space where the $n+1$ jet cross section saturates the rate for the hard process with n jets. As the p_T of the softest jet is lowered to values where $\sigma(n+1\ jet) \simeq \sigma(n\ jet)$, fixed order perturbation theory breaks down and multiple soft gluon emission (with resummation of collinear singularities into quark and gluon structure functions, etc.) needs to be considered in a full treatment. These refinements are beyond the scope of the present work. Instead we employ the truncated shower approximation (TSA) to normalize the higher order emission calculations [18]. The tree-level $n+1$ jet differential cross section $d\sigma(n+1\ j)_{TL}$ is replaced by

$$d\sigma(n+1\ j)_{TSA} = d\sigma(n+1\ j)_{TL}\left(1 - e^{-p_{Tj,min}^2/p_{TSA}^2}\right)\ , \tag{6}$$

with the parameter p_{TSA} properly chosen to correctly reproduce the lower order n jet cross section

when integrated over a given phase space region of this hard process. Here $p_{Tj,min}$ is the smallest transverse momentum of any of the final state massless partons. As $p_{Tj,min} \to 0$ the final factor in Eq. (6) acts as a regulator. Note that in the case of $t\bar{t}$ production the top and bottom quark transverse momenta are not included in the regularisation.

III. ISOLATING THE HEAVY HIGGS BOSON SIGNAL

Before discussing the minijet activity in signal and background events we first need to define the event selection in terms of requirements on hard leptons and jets. The purpose of these hard cuts is twofold: i) to reduce the various backgrounds while keeping a large fraction of signal events and ii) to make sure that the surviving background processes give very hard scattering events which will have a large transverse momentum scale for additional minijet activity.

We are interested in the decay of a very heavy Higgs boson, or, equivalently, in weak boson scattering at large center of mass energy and in the $J = 0$ partial wave. In either case the two charged W decay leptons will emerge with high transverse momentum, in the central region of the detector, and they will be well isolated. Thus we require the presence of two charged leptons ($\ell = e, \mu$) with

$$p_{T\ell} > 50\ GeV\ , \qquad |\eta_\ell| < 2\ , \qquad R_{\ell j} = \sqrt{(\eta_\ell - \eta_j)^2 + (\phi_\ell - \phi_j)^2} > 0.7\ . \tag{7}$$

Here $p_{T\ell}$ denotes the lepton transverse momentum and η_ℓ is its pseudorapidity. The $R_{\ell j} > 0.7$ separation cut forbids a parton (jet) of $p_T > 20$ GeV in a cone of radius 0.7 around the lepton direction. The lepton p_T cut in Eq. (7) is not in itself sufficient to focus on the production of two W's of large transverse momenta and large W-pair invariant mass. A variable which helps to substantially suppress W bremsstrahlung backgrounds is $\Delta p_{T\ell\ell}$, the difference of the charged lepton transverse momentum vectors [8]. We thus require

$$\Delta p_{T\ell\ell} = |p_{T\ell_1} - p_{T\ell_2}| > 300\,GeV\ , \qquad m_{\ell\ell} > 200\,GeV\ . \tag{8}$$

The additional cut on the dilepton invariant mass removes possible backgrounds from Z leptonic decays. It is largely superceded by the the $\Delta p_{T\ell\ell}$ cut, however.

Cross sections for events satisfying the lepton acceptance criteria of Eqs. (7,8) are listed in the first column of Table I for the case of a $m_H = 800$ GeV Higgs boson and the $q\bar{q} \to W^+W^-$ and $t\bar{t}$ production backgrounds. The weak boson scattering cross section for $m_H = 100$ GeV gives the electroweak background which is still contained in the $m_H = 800$ GeV line. Thus the signal cross section is defined as $B\sigma_{SIG} = B\sigma(m_H) - B\sigma(m_H = 100\ GeV)$. The 2.2 fb signal for $m_H = 800$ GeV retains about 50% of the total Higgs boson signal, with the reduction largely due to the stringent $\Delta p_{T\mu}$ cut.

The $qq \to qqH$ signal is further characterized by the presence of two forward quark jets. Typically only one of them emerges at substantial transverse momentum and hence we use single forward jet tagging. The tagging jet candidate is defined as the parton with the highest transverse momentum which satisfies the general jet definition criteria

$$p_{Tj} > 20\,GeV\ , \qquad |\eta_j| < 4.5\ , \qquad R_{jj} > 0.7\ . \tag{9}$$

Here the jet-jet separation cut is the parton level implementation of a jet definition cone with a radius of 0.7 in the legoplot. The tagging jet candidate is further required to fulfill

$$p_{Tj}^{tag} > 50\,GeV\ , \qquad E_j^{tag} > 500\,GeV\ , \qquad 1.5 < |\eta_j^{tag}| < 4.5\ . \tag{10}$$

While the signal can still be simulated at lowest order, we must include emission of an extra parton, *i.e.* consider W^+W^-j and $t\bar{t}j$ production in order to get a reliable background estimate. For the $t\bar{t}j$ cross section the tagging jet is occasionally one of the b-quark jets which results in a singular behavior of the cross section as the p_T of the extra parton approaches zero. This unphysical behavior is eliminated by using the TSA (see Eq. (6)) with $p_{TSA} = 20$ GeV which matches the $t\bar{t}j$ cross section to the $t\bar{t}$ cross section within the cuts of Eqs. (7,8). As can be seen by comparing the entries of the first two columns of table 1, requiring the presence of a tagging jet suppresses the backgrounds by about 1 order of magnitude while reducing the signal by 45%. This signal reduction is mostly due to the p_{Tj}^{tag} and E_j^{tag} requirements, which when taken alone, account for signal losses of about 0.4 fb and 0.6 fb respectively. Since the p_T distribution of the tagging jet is relatively soft for longitudinal weak boson scattering, one may contemplate

relaxing the p_{Tj}^{tag} cut if sufficient background reduction can be achieved by the minijet veto to be discussed later.

Another feature of the $qq \to qqH$ signal is the wide separation in pseudorapidity of the two final state quark jets from the leptons which arise in the Higgs boson decay. Imposing a minimal lepton tagging-jet separation,

$$min\ |\eta_j^{tag} - \eta_l| > 1.7\ , \tag{11}$$

reduces the backgrounds by more than a factor 2, with little loss for the signal (see Table I).

The hard cuts of Eqs. (7–11) define a trigger which selects events like the one sketched in the legoplot of Fig. 1. This trigger is about 22% efficient for a $m_H = 800$ GeV Higgs signal while reducing the QCD W^+W^- background to an acceptable level. Top production still drowns the signal, but can be suppressed by exploiting the b-quark jet activity. In a previous study it was shown that a veto on the centrally produced b quark jets above $p_{Tj}^{veto} = 25$ GeV is extremely effective in removing the $t\bar{t}$ background [6], but we have to be careful since at such low transverse momenta the production of minijets via the emission of additional gluons cannot be neglected at the LHC.

IV. MINIJET ACTIVITY

In order to study the minijet activity in the various processes we use the TSA and match $\sigma(n+1\ jet)_{TSA}$ to the lower order results within the hard cuts of Eqs. (7–11). This is achieved by setting $p_{TSA} = 63$ GeV for $\sigma(WW+2\ jet)$ and $p_{TSA} = 42$ GeV for $\sigma(t\bar{t}+2\ jet)$. For the weak boson scattering process $pp \to W^+W^-3j$, slightly different values of p_{TSA} are needed to match the $m_H = 100$ GeV and $m_H = 800$ GeV cross sections in the third column of table 1. Since this would lead to an incomplete subtraction of the electroweak background when determining the signal cross section $B\sigma_{SIG,TSA} = B\sigma(m_H)_{TSA} - B\sigma(m_H = 100\ GeV)_{TSA}$ we choose instead to match the $m_H = 800$ GeV signal rate of 1.02 fb in Table I which is achieved by setting $p_{TSA} = 7.3$ GeV.

The p_{TSA} parameter indicates the typical scale of minijet production. We therefore expect that moderate p_T minijet emission is much more likely for the backgrounds than for the signal process. The characteristic features of the additional jet activity, beyond the tagging jet, are displayed in Fig. 2. The pseudorapidity distributions of the jet closest to the lepton center $\overline{\eta} = (\eta_{\ell^+} + \eta_{\ell^-})/2$ are shown in Fig. 2(a). Here

$$\Delta\eta_{\ell j} = sign \cdot |\eta_j - \overline{\eta}| \,, \tag{12}$$

with the sign factor chosen such that the rapidity difference is counted as positive if the second jet is on the same side of the lepton center as the tagging jet (see Fig. 1). Figure 2(a) shows that emission of additional partons takes place in very different angular regions for the signal as compared to the backgrounds. In a $qq \to qqWW$ weak boson scattering event no color is being exchanged between the two scattering quarks which emerge in the forward and backward region. Color coherence between initial and final state radiation then leads to suppressed emission between these two jets. Due to the large WW invariant mass the decay products of the two W's emerge in the central region, however, and thus the additional jet activity is well separated from the charged leptons. Indeed the signal distribution, as given by the difference between the $m_H = 800$ GeV (solid) and the $m_H = 100$ GeV (dashed) curves in Fig. 2(a), is strikingly different from that of the backgrounds. The emission of soft gluons occurs mainly outside the interval defined by the two quark jets [12]. Consequently the jet closest to the lepton center is usually the second quark jet and not the soft gluon. This explains the asymmetric $\Delta\eta_{\ell j}$ distribution in Fig. 2(a): the large peak at negative values is due to the second quark jet. Gluon emission occuring close to the tagging jet and hence at positive $\Delta\eta_{\ell j}$ will rarely produce the jet closest to the two leptons.

In contrast to the signal the two background processes largely proceed by color octet exchange between the two incident partons and color coherence results in parton emission mainly in the central region. In $t\bar{t}$ production this effect is further enhanced by the b decay jets which cannot be too widely separated from the leptons since both arise from top quark decays. A veto against this central jet activity will clearly lead to a strong background reduction.

Figure 2(b) shows the probability to find at least one veto jet candidate above a certain minimal transverse momentum and in the vicinity of the leptons,

$$p_{Tj}^{veto} > p_{T,veto} \;, \qquad \eta_j^{veto} \varepsilon \; [\eta_\ell^{min} - 1.7, \eta_j^{tag}] \;\; or \;\; [\eta_j^{tag}, \eta_\ell^{max} + 1.7] \;, \tag{13}$$

(see shaded area of Fig. 1). This probability is determined by integrating $d\sigma_{TSA}/dp_{Tj}^{veto}$ and normalizing the result to the corresponding lower order cross section σ_{LO} within the cuts of Eqs. (7–11). The difference in veto probability between the $m_H = 800$ GeV signal and the two background processes is striking. In $t\bar{t}$ production the veto candidate is usually one of the b quarks ($\approx 80\%$ probability for $p_{T,veto} = 20$ GeV). In both $t\bar{t}$ and QCD W^+W^- production, minijet emission due to QCD radiation sets in at much larger transverse momenta than in the signal. This minijet p_T scale is about one to two orders of magnitude smaller than Q, the momentum transfer to the color charges which are accelerated in the hard scattering process. For the signal Q is the virtuality of the scattering weak bosons, *i.e.* $Q \approx m_W$ while the appropriate scale for the backgrounds is at least $Q = E_T(W)$ or $Q = E_T(t)$. As a result a given probability for minijet emission is reached at 5 to 10 times larger p_T scales in the backgrounds than in the signal.

In the truncated shower approximation only one soft parton is generated, with a finite probability to be produced outside the veto region of Eq. (13). The veto probability will therefore never reach 1, no matter how low a $p_{T,veto}$ is allowed. At small values of $p_{T,veto}$ we thus underestimate the veto probability because the TSA does not take into account multiple parton emission. In the soft region gluon emission dominates and one may assume that this soft gluon radiation approximately exponentiates. A rough estimate of multiple emission effects is thus provided by

$$P_{exp}(p_{T,veto}) = 1 - exp\left[-\frac{1}{\sigma_{LO}} \int_{p_{T,veto}}^{\infty} dp_{Tj}^{veto} \, \frac{d\sigma_{n+1}}{dp_{Tj}^{veto}}\right] \;, \tag{14}$$

where the unregularized $n+1$ parton cross section is integrated over the veto region of Eq. (13) and then normalized to the lower order cross section, σ_{LO}. For the QCD W^+W^-jj background the result of this exercise is shown as the dashed line in Fig. 2(b). It confirms the observations made before but the deviations from the TSA result also demonstrate the need for a quantitative calculation of the veto probability.

V. RAPIDITY GAPS AT THE MINIJET LEVEL

The prime concern of a veto strategy is to retain a high acceptance of signal events. Color coherence in the hard $qq \to qqH$ process leads to an almost complete absence of gluon radiation between the two quark jets [10,12] and hence to a rapidity gap in the distribution of hadrons which result from these soft gluons. In order to observe such a gap, however, no other sources of soft hadrons can be allowed, either from overlapping minimum bias events in a single bunch crossing at high luminosity or from the underlying event in a single pp collision. In the minijet model the latter is parameterized in terms of multiple parton scattering and only a few percent (given by the survival probability, P_s) of the signal events are expected to be free of multiple interactions [10,11,19]. Given the small weak boson scattering cross sections at the LHC (of order 100 fb), such a small signal acceptance makes a "traditional" rapidity gap selection infeasible.

We have seen above that the different gluon radiation patterns which are at the heart of a rapidity gap trigger become apparent in the distributions and the rate of minijets in the 20–50 GeV transverse momentum range. We are thus lead to define the rapidity gap trigger in terms of minijets instead of soft hadrons. Then the survival probability of the signal is determined as the complement to the probability that a minijet with $p_T > p_{T,veto}$ occurs in a random bunch crossing (overlapping events) or in the underlying event accompanying the hard scattering process. In both cases the survival probability is given by

$$P_s(p_{T,veto}) = 1 - \frac{\sigma_{jj}(p_{Tj} > p_{T,veto})}{\sigma_{eff}} \,. \tag{15}$$

Here $\sigma_{eff} = \mathcal{O}(25 \text{ mb})$ [20] for minijets produced in the underlying event and $\sigma_{eff} = [\mathcal{L}\ 25nsec]^{-1} = 4$ mb for overlapping events in a single bunch crossing at a luminosity of $\mathcal{L} = 10^{34} cm^{-2} sec^{-1}$. With single-jet cross sections of about 0.8 mb (2 mb) above $p_{Tj} = 20$ (15) GeV in the rapidity range of Eq. (13) the signal acceptance loss due to minijets in the underlying event appears to be acceptable down to transverse momenta of order 10–15 GeV while at $\mathcal{L} = 10^{34} cm^{-2} sec^{-1}$ overlapping events may produce random jets above 20 GeV p_T with about 20% probability. This estimate agrees with the results of a more detailed analysis of overlapping events at the LHC [21].

In the following we shall assume that a veto on minijets with $p_{T,veto} = 20$ GeV is feasible with little loss to the signal rate. Actually, it should be possible to significantly lower this transverse momentum cut. Central tracking may allow one to separate the z-vertex position of the hard trigger leptons from the interaction point of the minijet if the latter arises from an overlapping event. Assuming that the LHC interaction region will be about 10 cm long [22] a z-vertex resolution of the charged tracks inside the minijet of a few mm should suffice. Clearly, these questions should be addressed in experimental simulations. Here we just want to emphasize that an elimination of minijets from overlapping events and hence a lowering of $p_{T,veto}$ would greatly enhance background rejection with very little damage to the signal rate.

An estimate of the background reduction which can be achieved by vetoing additional jets above $p_{T,veto} = 20$ GeV is demonstrated by the last column in table 1. The minijet veto reduces the QCD WW background to a negligible level while leaving a $t\bar{t}$ background of about 0.5 fb. Notice that the top production background would be a factor two larger had we not taken into account the extra emission of soft partons in the $\mathcal{O}(\alpha_s^4)$ $t\bar{t}jj$ production process. Another measure of the background reduction is provided in Fig. 3 where we show the distribution in the lepton transverse momentum difference $\Delta p_{T\mathcal{U}}$, after our minijet veto. A cut at $\Delta p_{T\mathcal{U}} = 400$ GeV instead of the 300 GeV chosen in Eq. (8) would further reduce the background. However, trying to make a more stringent minijet veto experimentally feasible may be the more promising strategy.

VI. CONCLUSIONS

The angular distribution and the typical momentum scale of the minijet activity provide a powerful tool to distinguish the color structure of hard scattering events. In t-channel color singlet exchange, such as weak boson scattering events, there is a suppressed central minijet activity and the minijets in Higgs boson events typically carry transverse momenta well below 20 GeV. In contrast, backgrounds such as QCD W^+W^- or $t\bar{t}$ production involve the t-channel exchange of color octet gluons. This leads to strong minijet activity at central rapidities with $p_T \sim$ 20–50 GeV, which should be identifiable even in the high luminosity environment of the

LHC. Essentially, a minijet veto corresponds to a rapidity gap search at the semihard parton level which results in a large signal acceptance (or survival probability) even at high luminosity.

While a minijet veto appears to be a promising technique, many questions need to be answered before its full potential as a trigger for weak boson scattering events can be confirmed. The main question is detector related: how low a p_T threshold for the veto can be allowed without losing significantly on signal acceptance? Since background levels would be reduced dramatically if the veto threshold could be reduced to the 10–15 GeV range, the search strategy for a heavy Higgs boson depends crucially on what can finally be achieved experimentally. On the theoretical side it is necessary to improve the predictions for the minijet activity in a region which is at the limits of a perturbative treatment. The task is to preserve the color coherence of multiple soft and/or collinear parton emission while keeping the information on the momentum scale where multiple emission becomes important. Reliable calculations of these scales are essential to achieve a quantitative estimate of the background reduction factors due to a minijet veto. Clearly, a leading logarithm calculation, with an undetermined comparison scale, is insufficient.

The observation of these effects in very hard dijet events at the Tevatron should provide an invaluable source of information [23]. It should demonstrate the existence of enhanced minijet activity in hard QCD events and give an estimate of the relevant momentum scales. Since we are dealing with phenomena beyond the limits of fixed order perturbation theory, a fruitful interplay between experiment and theory appears to be the most promising way to turn minijet vetoing into a quantitative tool to search for a very heavy Higgs boson or to make weak boson scattering visible at future hadron colliders.

ACKNOWLEDGMENTS

We thank A. Stange for making his $t\bar{t}jj$ Monte Carlo program available to us and we are greatful to him and J. Ohnemus for comparisons of numerical results. This research was supported in part by the University of Wisconsin Research Committee with funds granted by the Wisconsin Alumni Research Foundation and in part by the U. S. Department of Energy under

Contract No. DE-AC02-76ER00881.

REFERENCES

[1] R. N. Cahn *et al.*, Phys. Rev. **D35**, 1626 (1987); V. Barger, T. Han, and R. J. N. Phillips, Phys. Rev. **D37** 2005 (1988); R. Kleiss and W. J. Stirling, Phys. Lett. **200B**, 193 (1988).

[2] D. Froideveaux, in *Proceedings of the ECFA Large Hadron Collider Workshop*, Aachen, Germany, 1990, edited by G. Jarlskog and D. Rein (CERN report 90-10, Geneva, Switzerland, 1990), Vol II, p. 444; M. H. Seymour, *ibid*, p. 557.

[3] U. Baur and E. W. N. Glover, Nucl. Phys. **B347**, 12 (1990); U. Baur and E. W. N. Glover, Phys. Lett.**B252**, 683 (1990).

[4] V. Barger, K. Cheung, T. Han, and R. J. N. Phillips, Phys. Rev. **D42**, 3052 (1990).

[5] V. Barger, K. Cheung, T. Han, J. Ohnemus, and D. Zeppenfeld, Phys. Rev. **D44**, 1426 (1991).

[6] V. Barger, K. Cheung, T. Han, and D. Zeppenfeld, Phys. Rev. **D44**, 2701 (1991); **48** 5444E (1993); **48**, 5433 (1993).

[7] V. Barger, K. Cheung, T. Han, A. Stange, and D. Zeppenfeld, Phys. Rev. **D46**, 2028 (1992).

[8] D. Dicus, J. F. Gunion, and R. Vega, Phys. Lett. **B258**, 475 (1991); D. Dicus, J. F. Gunion, L. H. Orr, and R. Vega, Nucl. Phys. **B377**, 31 (1991).

[9] Y. L. Dokshitzer, V. A. Khoze, and S. Troyan, in *Proceedings of the 6th International Conference on Physics in Collisions*, (1986) ed. M. Derrick (World Scientific, Singapore, 1987) p.365.

[10] J. D. Bjorken, Int. J. Mod. Phys. **A7**, 4189 (1992); Phys. Rev. **D47**, 101 (1993); preprint SLAC-PUB-5823 (1992).

[11] R. S. Fletcher and T. Stelzer, Phys. Rev. **D48**, 5162 (1993).

[12] A. Duff and D. Zeppenfeld, Phys. Rev. **D50**, 3204 (1994).

[13] A. D. Martin, R. G. Roberts, and W. J. Stirling, University of Durham Preprint DTP/94/34 (1994), Phys. Rev. **D**, in press.

[14] R. K. Ellis and J. C. Sexton, Nucl. Phys. **B282**, 642 (1987); P. Nason, S. Dawson, and R. K. Ellis, Nucl. Phys. **B303**, 607 (1988); W. Beenakker *et al.*, Phys. Rev. **D40**, 54 (1989); Nucl. Phys. **B351**, 507 (1991).

[15] A. Stange, private communication.

[16] V. Barger, T. Han, J. Ohnemus, and D. Zeppenfeld, Phys. Rev. **D41**, 2782 (1989). See references therein for earlier calculations of $pp \to W^+W^- + 0, 1$ jet production.

[17] J. Ohnemus, Phys. Rev. **D44**, 1403 (1991); **D50**, 1931 (1993).

[18] V. Barger and R. J. N. Phillips, Phys. Rev. Lett. **55**, 2752 (1985); H. Baer, V. Barger, H. Goldberg, and R. J. N. Phillips, Phys. Rev. **D37**, 3152 (1988).

[19] E. Gotsman, E. M. Levin, and U. Maor, Phys. Lett. **B309**, 199 (1993).

[20] CDF collaboration, F. Abe *et al.*, Phys. Rev. **D47**, 4857 (1993).

[21] G. Ciapetta and A. DiCiaccio, in *Proceedings of the ECFA Large Hadron Collider Workshop*, Aachen, Germany, 1990, edited by G. Jarlskog and D. Rein (CERN report 90-10, Geneva, Switzerland, 1990), Vol II, p. 155.

[22] CMS Collaboration, Letter of Intent, M. Markytan *et al.*, report CERN/LHCC 92-3 (1992).

[23] D. Summers and D. Zeppenfeld, in preparation.

TABLES

TABLE I. Signal and background cross sections $B\sigma$ in fb after increasingly stringent cuts. Four leptonic decay channels of the W^+W^- pair are included. The signal is defined as $\sigma(m_H) - \sigma(m_H = 100\ \text{GeV})$.

	lepton cuts only [Eq. (7)–(8)]	+ tagging jet [Eq. (10)]	+ lepton-tagging jet separation [Eq. (11)]	+ minijet veto ($p_{T,veto} =$ 20 GeV) [Eq. (13)]
$WW(jj)$	27.4	1.73	0.57	0.13
$t\bar{t}(jj)$	640	57	25	0.47
$m_H = 100$ GeV	1.18	0.56	0.29	0.18
$m_H = 800$ GeV	3.4	1.79	1.31	0.97
signal:				
$m_H = 600$ GeV				0.78
$m_H = 800$ GeV	2.2	1.23	1.02	0.79
$m_H = 1$ TeV				0.62

FIGURES

FIG. 1. Legoplot sketch of a typical event after the hard cuts of Eqs. (7–11). The shaded area represents the veto region defined in Eq. (13). $\overline{\eta}$ is the average pseudorapidity of the two charged leptons.

FIG. 2. Rapidity and transverse momentum distributions of secondary jets in $m_H = 800$ GeV $\mathcal{O}(\alpha_s)$ Higgs production (solid lines), $t\bar{t}jj$ production (dash-dotted lines) and QCD W^+W^-jj production (dotted lines). In a) $\Delta\eta_{\ell j}$ measures the pseudorapidity distance of the jet closest to the leptons from the average lepton rapidity $\bar{\eta}$. Also included is the distribution for the electroweak background as defined by the $m_H = 100$ GeV case (dashed line). The probability to find a veto jet candidate above a transverse momentum $p_{T,veto}$ in the veto region of Eq. (13) is shown in b). For QCD W^+W^-jj production the result for soft parton exponentiation is shown as the dashed line (see Eq. (14)).

FIG. 3. Dependence of signal and backgrounds on the transverse momentum difference of the two charged leptons. In addition to the cuts of Eqs. (7–11) a minijet veto within the veto region of Eq. (13) is imposed with $p_{T,veto} = 20$ GeV.

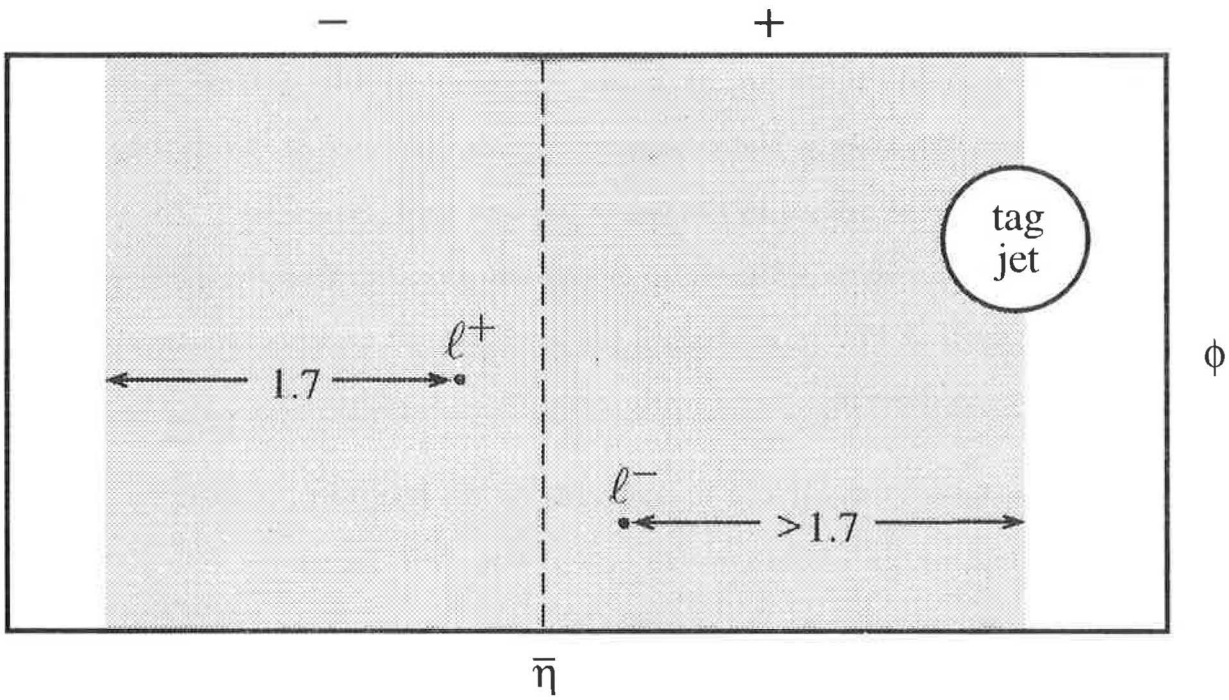

Fig. 1

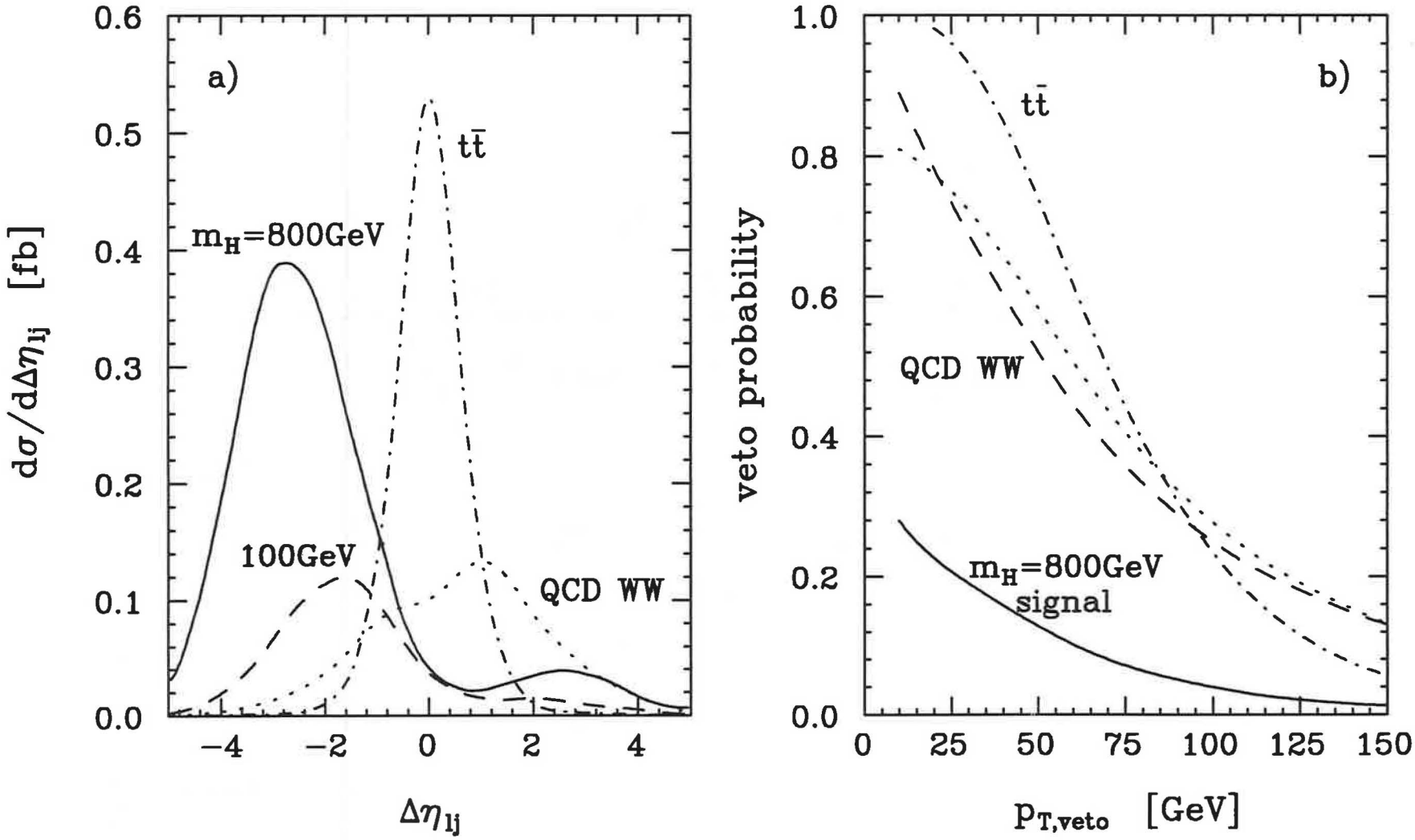
a)
b)
m_H=800GeV
$t\bar{t}$
100GeV
QCD WW
$d\sigma/d\Delta\eta_{lj}$ [fb]
$\Delta\eta_{lj}$
veto probability
m_H=800GeV
signal
$p_{T,veto}$ [GeV]

Fig. 2

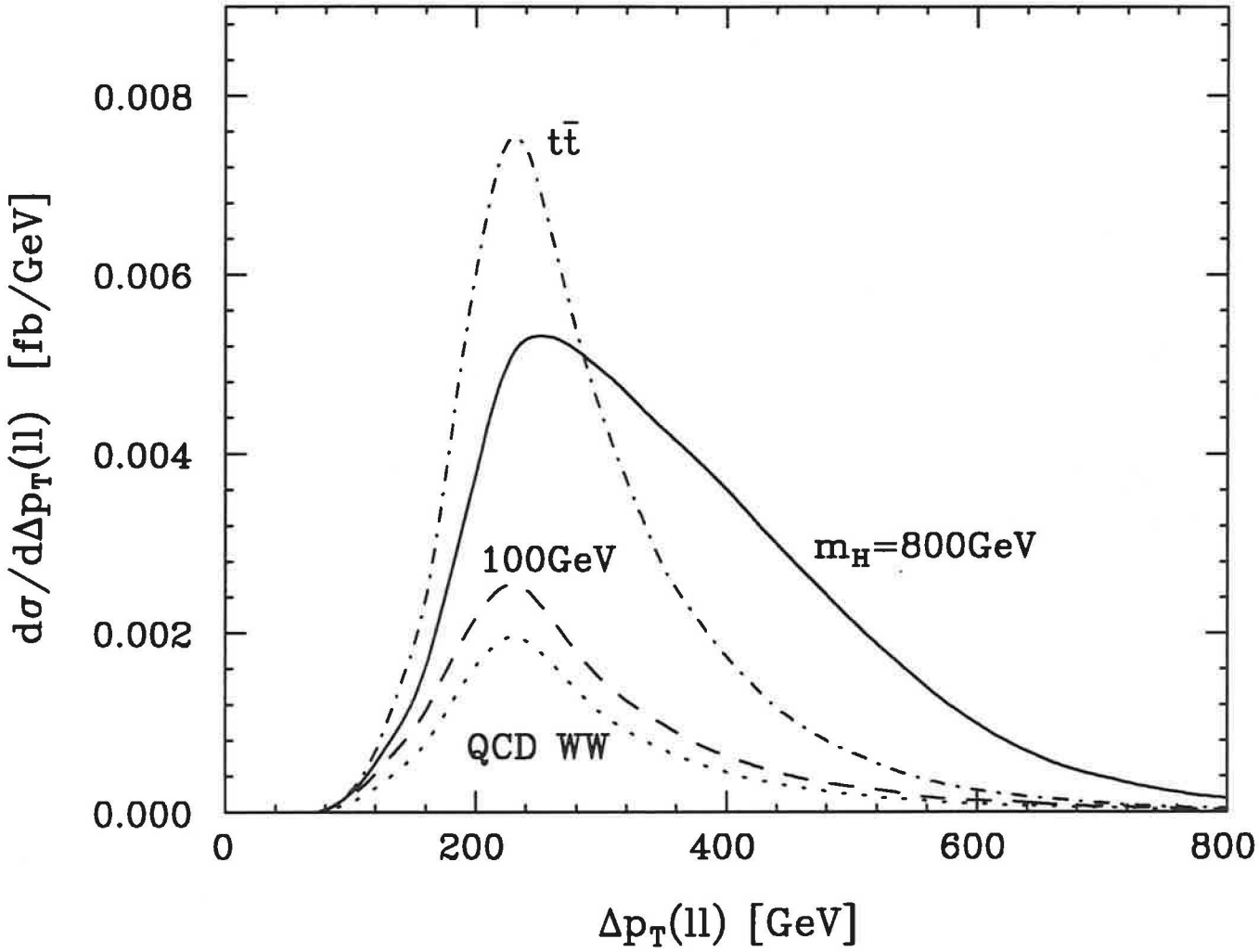
0.008
0.006
0.004
0.002
0.000
0
200
400
600
800
$t\bar{t}$
100GeV
m_H=800GeV
QCD WW
$d\sigma/d\Delta p_T(ll)$ [fb/GeV]
$\Delta p_T(ll)$ [GeV]

Fig. 3